SUPPLEMENTARY APPENDIX

Identification of novel microRNA signatures linked to acquired aplastic anemia

Kohei Hosokawa, Pawel Muranski, Xingmin Feng, Keyvan Keyvanfar, Danielle M. Townsley, Bogdan Dumitriu, Jichun Chen, Sachiko Kajigaya, James G. Taylor, Christopher S. Hourigan, A. John Barrett, and Neal S. Young

Hematology Branch, National Heart, Lung, and Blood Institute (NHLBI), NIH, Bethesda, Maryland, USA

 doi:10.3324/haematol.2015.126128
Manuscript received on March 5, 2015. Manuscript accepted on September 8, 2015.
Correspondence: kohei.hosokawa@nih.gov

Supplemental Data

Table S1. T cell and B cell Activation miRNA PCR Array in human and mouse

	human (MIHS-111Z)		mouse (MIMM-111Z)	
	miRBase Accession No.	human mature miRNA	miRBase Accession No.	mouse mature miRNA
1	MIMAT0000062	hsa-let-7a-5p	MIMAT0000521	mmu-let-7a-5p
2	MIMAT0000063	hsa-let-7b-5p	MIMAT0000523	mmu-let-7c-5p
3	MIMAT0000064	hsa-let-7c-5p	MIMAT0000383	mmu-let-7d-5p
4	MIMAT0000065	hsa-let-7d-5p	MIMAT0000524	mmu-let-7e-5p
5	MIMAT0000066	hsa-let-7e-5p	MIMAT0000525	mmu-let-7f-5p
6	MIMAT0000067	hsa-let-7f-5p	MIMAT0000121	mmu-let-7g-5p
7	MIMAT0000414	hsa-let-7g-5p	MIMAT0000122	mmu-let-7i-5p
8	MIMAT0000415	hsa-let-7i-5p	MIMAT0000133	mmu-miR-101a-3p
9	MIMAT0000098	hsa-miR-100-5p	MIMAT0000616	mmu-miR-101b-3p
10	MIMAT0000099	hsa-miR-101-3p	MIMAT0000546	mmu-miR-103-3p
11	MIMAT0000680	hsa-miR-106b-5p	MIMAT0000385	mmu-miR-106a-5p
12	MIMAT0000423	hsa-miR-125b-5p	MIMAT0000386	mmu-miR-106b-5p
13	MIMAT0000445	hsa-miR-126-3p	MIMAT0005837	mmu-miR-1187
14	MIMAT0000424	hsa-miR-128-3p	MIMAT0005857	mmu-miR-1196-5p
15	MIMAT0000691	hsa-miR-130b-3p	MIMAT0000136	mmu-miR-125b-5p
16	MIMAT0000426	hsa-miR-132-3p	MIMAT0000138	mmu-miR-126a-3p
17	MIMAT0000250	hsa-miR-139-5p	MIMAT0000387	mmu-miR-130b-3p
18	MIMAT0000434	hsa-miR-142-3p	MIMAT0000656	mmu-miR-139-5p
19	MIMAT0000433	hsa-miR-142-5p	MIMAT0000155	mmu-miR-142a-3p
20	MIMAT0000437	hsa-miR-145-5p	MIMAT0000154	mmu-miR-142a-5p
21	MIMAT0000449	hsa-miR-146a-5p	MIMAT0000157	mmu-miR-145a-5p
22	MIMAT0002809	hsa-miR-146b-5p	MIMAT0000158	mmu-miR-146a-5p
23	MIMAT0000251	hsa-miR-147a	MIMAT0003475	mmu-miR-146b-5p
24	MIMAT0000243	hsa-miR-148a-3p	MIMAT0000160	mmu-miR-150-5p
25	MIMAT0000451	hsa-miR-150-5p	MIMAT0000165	mmu-miR-155-5p
26	MIMAT0000646	hsa-miR-155-5p	MIMAT0000526	mmu-miR-15a-5p
27	MIMAT0000068	hsa-miR-15a-5p	MIMAT0004624	mmu-miR-15a-3p
28	MIMAT0004488	hsa-miR-15a-3p	MIMAT0000124	mmu-miR-15b-5p
29	MIMAT0000417	hsa-miR-15b-5p	MIMAT0000527	mmu-miR-16-5p
30	MIMAT0000069	hsa-miR-16-5p	MIMAT0000649	mmu-miR-17-5p
31	MIMAT0000070	hsa-miR-17-5p	MIMAT0000210	mmu-miR-181a-5p
32	MIMAT0000071	hsa-miR-17-3p	MIMAT0000673	mmu-miR-181b-5p
33	MIMAT0000256	hsa-miR-181a-5p	MIMAT0000211	mmu-miR-182-5p
34	MIMAT0000257	hsa-miR-181b-5p	MIMAT0000213	mmu-miR-184-3p
35	MIMAT0000258	hsa-miR-181c-5p	MIMAT0000225	mmu-miR-195a-5p
36	MIMAT0002821	hsa-miR-181d-5p	MIMAT0000651	mmu-miR-19a-3p
37	MIMAT0000259	hsa-miR-182-5p	MIMAT0000513	mmu-miR-19b-3p
38	MIMAT0000454	hsa-miR-184	MIMAT0000529	mmu-miR-20a-5p
39	MIMAT0000072	hsa-miR-18a-5p	MIMAT0003187	mmu-miR-20b-5p
40	MIMAT0000440	hsa-miR-191-5p	MIMAT0000530	mmu-miR-21a-5p
41	MIMAT0000461	hsa-miR-195-5p	MIMAT0000661	mmu-miR-214-3p
42	MIMAT0000231	hsa-miR-199a-5p	MIMAT0000669	mmu-miR-221-3p
43	MIMAT0000073	hsa-miR-19a-3p	MIMAT0000665	mmu-miR-223-3p
44	MIMAT0000074	hsa-miR-19b-3p	MIMAT0000532	mmu-miR-23a-3p
45	MIMAT0000265	hsa-miR-204-5p	MIMAT0000125	mmu-miR-23b-3p
46	MIMAT0000075	hsa-miR-20a-5p	MIMAT0000219	mmu-miR-24-3p
47	MIMAT0001413	hsa-miR-20b-5p	MIMAT0000652	mmu-miR-25-3p
48	MIMAT0000076	hsa-miR-21-5p	MIMAT0000533	mmu-miR-26a-5p
49	MIMAT0000267	hsa-miR-210-3p	MIMAT0000534	mmu-miR-26b-5p
50	MIMAT0000271	hsa-miR-214-3p	MIMAT0000537	mmu-miR-27a-3p
51	MIMAT0000278	hsa-miR-221-3p	MIMAT0000126	mmu-miR-27b-3p
52	MIMAT0000279	hsa-miR-222-3p	MIMAT0000653	mmu-miR-28a-5p
53	MIMAT0000280	hsa-miR-223-3p	MIMAT0000535	mmu-miR-29a-3p
54	MIMAT0000078	hsa-miR-23a-3p	MIMAT0000127	mmu-miR-29b-3p
55	MIMAT0000418	hsa-miR-23b-3p	MIMAT0000536	mmu-miR-29c-3p
56	MIMAT0000080	hsa-miR-24-3p	MIMAT0000128	mmu-miR-30a-5p
57	MIMAT0000081	hsa-miR-25-3p	MIMAT0000130	mmu-miR-30b-5p
58	MIMAT0000082	hsa-miR-26a-5p	MIMAT0000514	mmu-miR-30c-5p
59	MIMAT0000083	hsa-miR-26b-5p	MIMAT0000248	mmu-miR-30e-5p
60	MIMAT0000084	hsa-miR-27a-3p	MIMAT0000538	mmu-miR-31-5p
61	MIMAT0000419	hsa-miR-27b-3p	MIMAT0000666	mmu-miR-320-3p
62	MIMAT0000085	hsa-miR-28-5p	MIMAT0000559	mmu-miR-326-3p
63	MIMAT0000086	hsa-miR-29a-3p	MIMAT0000571	mmu-miR-331-3p
64	MIMAT0000100	hsa-miR-29b-3p	MIMAT0000590	mmu-miR-342-3p
65	MIMAT0000681	hsa-miR-29c-3p	MIMAT0000597	mmu-miR-346-5p
66	MIMAT0000087	hsa-miR-30a-5p	MIMAT0000711	mmu-miR-365-3p
67	MIMAT0000420	hsa-miR-30b-5p	MIMAT0004882	mmu-miR-466f-3p
68	MIMAT0000244	hsa-miR-30c-5p	MIMAT0004881	mmu-miR-466f-5p
69	MIMAT0000245	hsa-miR-30d-5p	MIMAT0004883	mmu-miR-466g
70	MIMAT0000692	hsa-miR-30e-5p	MIMAT0004884	mmu-miR-466h-5p
71	MIMAT0000089	hsa-miR-31-5p	MIMAT0005848	mmu-miR-466j
72	MIMAT0000756	hsa-miR-326	MIMAT0003478	mmu-miR-467b-3p
73	MIMAT0000760	hsa-miR-331-3p	MIMAT0005846	mmu-miR-467f
74	MIMAT0000765	hsa-miR-335-5p	MIMAT0004782	mmu-miR-483-5p
75	MIMAT0000753	hsa-miR-342-3p	MIMAT0004894	mmu-miR-574-3p
76	MIMAT0000773	hsa-miR-346	MIMAT0004893	mmu-miR-574-5p
77	MIMAT0000255	hsa-miR-34a-5p	MIMAT0005853	mmu-miR-669e-5p
78	MIMAT0000710	hsa-miR-365a-3p	MIMAT0005839	mmu-miR-669f-3p
79	MIMAT0004748	hsa-miR-423-5p	MIMAT0009421	mmu-miR-669o-5p
80	MIMAT0003239	hsa-miR-574-3p	MIMAT0003735	mmu-miR-672-5p
81	MIMAT0000092	hsa-miR-92a-3p	MIMAT0003505	mmu-miR-714
82	MIMAT0000093	hsa-miR-93-5p	MIMAT0003892	mmu-miR-762
83	MIMAT0000096	hsa-miR-98-5p	MIMAT0000540	mmu-miR-93-5p
84	MIMAT0000097	hsa-miR-99a-5p	MIMAT0000545	mmu-miR-98-5p

Table S2. Custom RT² Profiler™ microRNA Targets PCR Arrays

Gene Symbol	Accession Number	Description		Validated Targeted By	PubMed IDs	PubMed IDs	PubMed IDs
ADAM17	NM_003183	ADAM metallopeptidase domain 17	Experimenally validated	miR-145-5p	23441135		
ADAM9	NM_003816	ADAM metallopeptidase domain 9	Experimenally validated	miR-126-3p	23437250		
AKT1	NM_005163	V-akt murine thymoma viral oncogene homolog 1	Experimenally validated	miR-126-3p	23142521		
AKT2	NM_001626	V-akt murine thymoma viral oncogene homolog 2	Experimenally validated	miR-126-3p	23142521		
BNIP3	NM_004052	BCL2/adenovirus E1B 19kDa interacting protein 3	Experimenally validated	miR-145-5p	20332243		
CBFB	NM_001755	Core-binding factor, beta subunit	Experimenally validated	miR-145-5p	19915607		
CD28	NM_006139	CD28 molecule	Experimenally validated	miR-145-5p	24043548		
CHUK	NM_001278	Conserved helix-loop-helix ubiquitous kinase	Experimenally validated	miR-223-3p	20711193		
CLINT1	NM_014666	Clathrin interactor 1	Experimenally validated	miR-145-5p	19915607		
CRK	NM_016823	V-crk sarcoma virus CT10 oncogene homolog (avian)	Experimenally validated	miR-126-3p	18602365	20619534	
CTGF	NM_001901	Connective tissue growth factor	Experimenally validated	miR-145-5p	23390502		
CXCL12	NM_000609	Chemokine (C-X-C motif) ligand 12	Experimenally validated	miR-126-3p	23396050		
DDR1	NM_001954	Discoidin domain receptor tyrosine kinase 1	Experimenally validated	miR-199a-5p	20799954		
DNMT1	NM_001379	DNA (cytosine-5-)-methyltransferase 1	Experimenally validated	miR-126-3p	21538319		
E2F1	NM_005225	E2F transcription factor 1	Experimenally validated	miR-223-3p	20029046		
ERG	NM_182918	V-ets erythroblastosis virus E26 oncogene homolog (avian)	Experimenally validated	miR-145-5p	23480797		
ETS1	NM_005238	V-ets erythroblastosis virus E26 oncogene homolog 1 (avian)	Experimenally validated	miR-199a-5p	23060436		
EZH2	NM_004456	Enhancer of zeste homolog 2 (Drosophila)	Experimenally validated	miR-199a-5p	19818710		
FBXW7	NM_033632	F-box and WD repeat domain containing 7	Experimenally validated	miR-223-3p	22270966		
FLI1	NM_002017	Friend leukemia virus integration 1	Experimenally validated	miR-145-5p	20382729	20737575	21217773
FOXO1	NM_002015	Forkhead box O1	Experimenally validated	miR-223-3p	22569260		
FOXO3	NM_001455	Forkhead box O3	Predicted	miR-126-3p,miR-223-3p			
FSCN1	NM_003088	Fascin homolog 1, actin-bundling protein (Strongylocentrotus purpuratus)	Experimenally validated	miR-145-5p	20160723	21351259	21258769
GSK3B	NM_002093	Glycogen synthase kinase 3 beta	Experimenally validated	miR-126-3p	23142521		
GZMB	NM_004131	Granzyme B (granzyme 2, cytotoxic T-lymphocyte-associated serine esterase 1)	Predicted	miR-199a-5p			
HDAC2	NM_001527	Histone deacetylase 2	Experimenally validated	miR-145-5p	23499894		
HIF1A	NM_001530	Hypoxia inducible factor 1, alpha subunit (basic helix-loop-helix transcription factor)	Experimenally validated	miR-199a-5p	22383663		
HOXA9	NM_152739	Homeobox A9	Experimenally validated	miR-126-3p	18474618		
HSP90B1	NM_003299	Heat shock protein 90kDa beta (Grp94), member 1	Experimenally validated	miR-223-3p	23208072		
IFNB1	NM_002176	Interferon, beta 1, fibroblast	Experimenally validated	miR-145-5p	20130213		
IGF1R	NM_000875	Insulin-like growth factor 1 receptor	Experimenally validated	miR-223-3p	22073238		
IGFBP2	NM_000597	Insulin-like growth factor binding protein 2, 36kDa	Experimenally validated	miR-126-3p	22170610		
IKBKB	NM_001556	Inhibitor of kappa light polypeptide gene enhancer in B-cells, kinase beta	Experimenally validated	miR-199a-5p	18408758		
IL18R1	NM_003855	Interleukin 18 receptor 1	Predicted	miR-145-5p			
IL21R	NM_021798	Interleukin 21 receptor	Predicted	miR-126-3p			
IL12RB2	NM_001559	Interleukin 12 receptor, beta 2	Predicted	miR-199a-5p			
IRS1	NM_005544	Insulin receptor substrate 1	Experimenally validated	miR-145-5p	17827156	19391107	22431718
IRS2	NM_003749	Insulin receptor substrate 2	Experimenally validated	miR-145-5p	22431718		
KLF4	NM_004235	Kruppel-like factor 4 (gut)	Experimenally validated	miR-145-5p	19409607		
KRAS	NM_004985	V-Ki-ras2 Kirsten rat sarcoma viral oncogene homolog	Experimenally validated	miR-126-3p	22384141		
LIF	NM_002309	Leukemia inhibitory factor (cholinergic differentiation factor)	Experimenally validated	miR-199a-5p	19011087		
LMO2	NM_005574	LIM domain only 2 (rhombotin-like 1)	Experimenally validated	miR-223-3p	19278969	19017354	
MAP3K11	NM_002419	Mitogen-activated protein kinase kinase kinase 11	Experimenally validated	miR-199a-5p	21048306		
MDM2	NM_002392	Mdm2 p53 binding protein homolog (mouse)	Experimenally validated	miR-145-5p	22330136		
MERTK	NM_006343	C-mer proto-oncogene tyrosine kinase	Experimenally validated	miR-126-3p	22170610		
MMP7	NM_002423	Matrix metallopeptidase 7 (matrilysin, uterine)	Experimenally validated	miR-126-3p	23437250		
MYC	NM_002467	V-myc myelocytomatosis viral oncogene homolog (avian)	Experimenally validated	miR-145-5p	19202062	21092188	
NANOG	NM_024865	Nanog homeobox	Experimenally validated	miR-145-5p	23541921		
NFATC1	NM_172390	Nuclear factor of activated T-cells, cytoplasmic, calcineurin-dependent 1	Experimenally validated	miR-145-5p	24043548		
NFIA	NM_005595	Nuclear factor I/A	Experimenally validated	miR-223-3p	16325577		
NLRP3	NM_183395	NLR family, pyrin domain containing 3	Experimenally validated	miR-223-3p	22984082		
NRAS	NM_002524	Neuroblastoma RAS viral (v-ras) oncogene homolog	Experimenally validated	miR-145-5p	23201159		
PAK4	NM_005884	P21 protein (Cdc42/Rac)-activated kinase 4	Experimenally validated	miR-145-5p	22766504		
PARP1	NM_001618	Poly (ADP-ribose) polymerase 1	Experimenally validated	miR-223-3p	23757351		
PIK3CD	NM_005026	Phosphoinositide-3-kinase, catalytic, delta polypeptide	Experimenally validated	miR-126-3p	23142521		
PIK3R2	NM_005027	Phosphoinositide-3-kinase, regulatory subunit 2 (beta)	Experimenally validated	miR-126-3p	18987025	18663744	21249429
PITPNC1	NM_181671	Phosphatidylinositol transfer protein, cytoplasmic 1	Experimenally validated	miR-126-3p	22170610		
PLK2	NM_006622	Polo-like kinase 2	Experimenally validated	miR-126-3p	18832181		
POU5F1	NM_002701	POU class 5 homeobox 1	Experimenally validated	miR-145-5p	19409607	21496429	23541921
PPP3CA	NM_000944	Protein phosphatase 3, catalytic subunit, alpha isozyme	Experimenally validated	miR-145-5p	19915607		
PTPN9	NM_002833	Protein tyrosine phosphatase, non-receptor type 9	Experimenally validated	miR-126-3p	21163928		
RHOB	NM_004040	Ras homolog gene family, member B	Experimenally validated	miR-223-3p	19850724		
ROBO2	NM_002942	Roundabout, axon guidance receptor, homolog 2 (Drosophila)	Experimenally validated	miR-145-5p	21276775		
SERPINE1	NM_000602	Serpin peptidase inhibitor, clade E (nexin, plasminogen activator inhibitor type 1), member 1	Experimenally validated	miR-145-5p	22108519		
SLC7A5	NM_003486	Solute carrier family 7 (amino acid transporter light chain, L system), member 5	Experimenally validated	miR-126-3p	21439283		
SMAD4	NM_005359	SMAD family member 4	Experimenally validated	miR-199a-5p	22821565		
SMARCA2	NM_003070	WI/SNF related, matrix associated, actin dependent regulator of chromatin, subfamily a, member	Experimenally validated	miR-199a-5p	21189327		
SOCS7	NM_014598	Suppressor of cytokine signaling 7	Experimenally validated	miR-145-5p	23392170		
SOX2	NM_003106	SRY (sex determining region Y)-box 2	Experimenally validated	miR-145-5p	19409607	23541921	
SP3	NM_003111	Sp3 transcription factor	Experimenally validated	miR-223-3p	22080513		
SPRED1	NM_152594	Sprouty-related, EVH1 domain containing 1	Experimenally validated	miR-126-3p	18987025	18694566	22525256
STAT1	NM_007315	Signal transducer and activator of transcription 1, 91kDa	Experimenally validated	miR-145-5p	23199328		
STMN1	NM_005563	Stathmin 1	Experimenally validated	miR-223-3p	18555017	22470493	
SWAP70	NM_015055	SWAP switching B-cell complex 70kDa subunit	Experimenally validated	miR-145-5p	21360565		
TGFBR1	NM_004612	Transforming growth factor, beta receptor 1	Predicted	miR-145-5p			
TGFBR2	NM_003242	Transforming growth factor, beta receptor II (70/80kDa)	Predicted	miR-145-5p			
TIRAP	NM_001039661	Toll-interleukin 1 receptor (TIR) domain containing adaptor protein	Experimenally validated	miR-145-5p	19898489		
TLR4	NM_138554	Toll-like receptor 4	Predicted	miR-145-5p			
TNFRSF10A	NM_003844	Tumor necrosis factor receptor superfamily, member 10a	Predicted	miR-126-3p,miR-145-5p			
TNFRSF10B	NM_003842	Tumor necrosis factor receptor superfamily, member 10b	Predicted	miR-145-5p			
TOM1	NM_005488	Target of myb1 (chicken)	Experimenally validated	miR-126-3p	20083669		
VCAM1	NM_001078	Vascular cell adhesion molecule 1	Experimenally validated	miR-126-3p	18227515		
VEGFA	NM_003376	Vascular endothelial growth factor A	Experimenally validated	miR-126-3p	19223090	22510476	21249429
YES1	NM_005433	V-yes-1 Yamaguchi sarcoma viral oncogene homolog 1	Experimenally validated	miR-145-5p	20098684		
ACTB	NM_001101	Actin, beta	NA	NA	NA		
B2M	NM_004048	Beta-2-microglobulin	NA	NA	NA		
GAPDH	NM_002046	Glyceraldehyde-3-phosphate dehydrogenase	NA	NA	NA		
HPRT1	NM_000194	Hypoxanthine phosphoribosyltransferase 1	NA	NA	NA		
RPLP0	NM_001002	Ribosomal protein, large, P0	NA	NA	NA		
HGDC	SA_00105	Human Genomic DNA Contamination	NA	NA	NA		
RTC	SA_00104	Reverse Transcription Control	NA	NA	NA		
PPC	SA_00103	Positive PCR Control	NA	NA	NA		

Table S3. Fold change and *P* values in miRNA PCR array

List of miRNAs significantly (p <0.01) downregulated (> 3 FC) in lymphocyte subset in AA

CD4$^+$ T cells

Mature ID	Fold change (AA/Controls)	*p* value
hsa-miR-126-3p	0.07	0.000086
hsa-miR-145-5p	0.17	0.000047
hsa-miR-199a-5p	0.11	0.00001
hsa-miR-223-3p	0.28	0.005575

CD8$^+$ T cells

Mature ID	Fold change (AA/Controls)	*p* value
hsa-miR-126-3p	0.29	0.00074
hsa-miR-145-5p	0.22	0.000004
hsa-miR-199a-5p	0.16	0
hsa-miR-223-3p	0.28	0.002393

CD19$^+$ B cells

Mature ID	Fold change (AA/Controls)	*p* value
hsa-miR-126-3p	0.04	0.00001
hsa-miR-145-5p	0.34	0.000264
hsa-miR-199a-5p	0.12	0.000055

List of miRNAs significantly (p <0.01) upregulated or downregulated (> 3 FC) in lymphocyte subset in MDS

CD4$^+$ T cells

Mature ID	Fold change (MDS/Controls)	*p* value
hsa-miR-182-5p	4.38	0.002769
hsa-miR-142-5p	0.19	0.000299
hsa-miR-199a-5p	0.12	0.000435
hsa-miR-19a-3p	0.25	0.001563

CD8$^+$ T cells

Mature ID	Fold change (MDS/Controls)	*p* value
hsa-miR-182-5p	4.71	0.001447
hsa-miR-34a-5p	3.02	0.002352
hsa-miR-574-3p	4.11	0.001924
hsa-miR-126-3p	0.16	0.002771
hsa-miR-199a-5p	0.11	0.000157
hsa-miR-19a-3p	0.27	0.001367
hsa-miR-19b-3p	0.33	0.000046
hsa-miR-223-3p	0.28	0.00037

List of miRNAs significantly (p <0.01) upregulated or downregulated (> 3 FC) in lymphocyte subset in SCD

CD4$^+$ T cells

Mature ID	Fold change (SCD/Controls)	*p* value
hsa-miR-34a-5p	3.9	0.000048
hsa-miR-142-3p	0.31	0.008815
hsa-miR-142-5p	0.16	0.000233
hsa-miR-199a-5p	0.27	0.001542
hsa-miR-19a-3p	0.26	0.002473
hsa-miR-19b-3p	0.24	0.00078

CD8$^+$ T cells

Mature ID	Fold change (SCD/Controls)	*p* value
hsa-miR-182-5p	3.53	0.000913
hsa-miR-34a-5p	3	0.00198
hsa-miR-101-3p	0.23	0.0082
hsa-miR-142-5p	0.19	0.004073
hsa-miR-199a-5p	0.25	0.00074

List of miRNAs significantly (p <0.05) upregulated or downregulated (> 2 FC) in lymphocyte subset in BMF mouse

CD4$^+$ T cells

Mature ID	Fold change (BMF/Controls)	*p* value
mmu-miR-103-3p	2.09	0.005779
mmu-miR-1196-5p	5.11	0.001963
mmu-miR-125b-5p	4.54	0.004136
mmu-miR-126a-3p	2.8	0.025158
mmu-miR-130b-3p	3.13	0.003907
mmu-miR-145a-5p	7.8	0.0002
mmu-miR-146a-5p	6.91	0.026675
mmu-miR-146b-5p	9.12	0.003031
mmu-miR-155-5p	8.46	0.000204
mmu-miR-15a-3p	2.77	0.040257
mmu-miR-182-5p	27.7	0.002052
mmu-miR-21a-5p	5.24	0.016754
mmu-miR-214-3p	7.66	0.001706
mmu-miR-221-3p	19.1	0
mmu-miR-223-3p	31.7	0.020176
mmu-miR-23b-3p	2.66	0.012983
mmu-miR-27b-3p	2.04	0.008408
mmu-miR-31-5p	4.92	0.006577
mmu-miR-365-3p	3.81	0.001121
mmu-miR-466f-3p	2.42	0.035638
mmu-miR-574-3p	2.87	0.0115
mmu-miR-714	4.3	0.008166
mmu-let-7c-5p	0.25	0.01051
mmu-let-7e-5p	0.43	0.021228
mmu-let-7f-5p	0.46	0.008926
mmu-let-7g-5p	0.28	0.000137
mmu-miR-101a-3p	0.16	0.000605
mmu-miR-101b-3p	0.26	0.000386
mmu-miR-139-5p	0.4	0.005717
mmu-miR-142a-3p	0.4	0.010775
mmu-miR-142a-5p	0.35	0.022693
mmu-miR-15b-5p	0.38	0.024745
mmu-miR-16-5p	0.43	0.018067
mmu-miR-181a-5p	0.12	0.000705
mmu-miR-19a-3p	0.21	0.008716
mmu-miR-19b-3p	0.22	0.000362
mmu-miR-20b-5p	0.43	0.011608
mmu-miR-26a-5p	0.33	0.02894
mmu-miR-26b-5p	0.24	0.0009
mmu-miR-29a-3p	0.3	0.009188
mmu-miR-29b-3p	0.25	0.004443
mmu-miR-29c-3p	0.24	0.000234
mmu-miR-30a-5p	0.47	0.000941
mmu-miR-30b-5p	0.26	0.000745
mmu-miR-30e-5p	0.47	0.000938
mmu-miR-342-3p	0.48	0.004355
mmu-miR-466g	0.22	0.000634
mmu-miR-466h-5p	0.19	0.011892
mmu-miR-466j	0.19	0.000006
mmu-miR-467b-3p	0.18	0.003025
mmu-miR-467f	0.27	0.00508
mmu-miR-669e-5p	0.13	0.000437
mmu-miR-669f-3p	0.31	0.000923
mmu-miR-669o-5p	0.23	0.00174

CD8$^+$ T cells

Mature ID	Fold change (BMF/Controls)	*p* value
mmu-miR-1187	6.61	0.036848
mmu-miR-1196-5p	11.1	0.008886
mmu-miR-125b-5p	6.19	0.046316
mmu-miR-126a-3p	3.99	0.001199
mmu-miR-130b-3p	3.38	0.001437
mmu-miR-145a-5p	9.31	0.008462
mmu-miR-146a-5p	9.22	0.000043
mmu-miR-146b-5p	11.6	0.000641
mmu-miR-155-5p	8.89	0.000301
mmu-miR-15a-3p	4.57	0.000144
mmu-miR-182-5p	37.9	0.000006
mmu-miR-21a-5p	15.7	0.000186
mmu-miR-214-3p	18.5	0.000599
mmu-miR-221-3p	9.33	0.000194
mmu-miR-346-5p	11.5	0.001938
mmu-miR-365-3p	4.61	0.00002
mmu-miR-466f-3p	5.61	0.000054
mmu-miR-483-5p	9.53	0.000753
mmu-miR-574-5p	4.1	0.000997
mmu-miR-672-5p	14.8	0.003064
mmu-miR-714	7.63	0.000437
mmu-miR-762	5.68	0.026325
mmu-let-7c-5p	0.16	0.007125
mmu-let-7e-5p	0.44	0.0044
mmu-let-7f-5p	0.4	0.006003
mmu-miR-101a-3p	0.09	0.000516
mmu-miR-101b-3p	0.14	0.00001
mmu-miR-139-5p	0.2	0.000008
mmu-miR-142a-3p	0.39	0.007036
mmu-miR-142a-5p	0.33	0.000249
mmu-miR-16-5p	0.49	0.012374
mmu-miR-181a-5p	0.15	0.000566
mmu-miR-19a-3p	0.29	0.000555
mmu-miR-19b-3p	0.23	0.000325
mmu-miR-23a-3p	0.41	0.000001
mmu-miR-26a-5p	0.26	0.001735
mmu-miR-26b-5p	0.21	0.002233
mmu-miR-27a-3p	0.23	0.000016
mmu-miR-29a-3p	0.25	0.000248
mmu-miR-29b-3p	0.14	0.000521
mmu-miR-29c-3p	0.2	0
mmu-miR-30b-5p	0.27	0.000582
mmu-miR-342-3p	0.3	0.000447
mmu-miR-466g	0.28	0.000151
mmu-miR-466h-5p	0.19	0.000683
mmu-miR-466j	0.2	0.000117
mmu-miR-467b-3p	0.23	0.011957
mmu-miR-467f	0.36	0.003069
mmu-miR-669e-5p	0.04	0.011612
mmu-miR-669f-3p	0.21	0.00073
mmu-miR-669o-5p	0.12	0.001013

Table S4. Pathways linked to the four significantly downregulated miRNAs in AA patients

KEGG pathway	*p*-value	number of genes	gene list	number of miRNAs	miRNA list
Hepatitis B	5.31E-10	12	E2F1,PIK3R2,IFNB1,CHUK,IKBKB,CCNE2,E2F3,TIRAP,MYC,CDKN1A,IL6,STAT1	4	miR-126-3p,miR-145-5p,miR-199a-5p,miR-223-3p
Osteoclast differentiation	2.70E-08	9	PIK3R2,IFNB1,CHUK,SQSTM1,MAP2K6,IKBKB,PPP3CA,JUNB,STAT1	4	miR-126-3p,miR-145-5p,miR-199a-5p,miR-223-3p
Toll-like receptor signaling pathway	2.70E-08	8	PIK3R2,IFNB1,CHUK,MAP2K6,IKBKB,TIRAP,IL6,STAT1	4	miR-126-3p,miR-145-5p,miR-199a-5p,miR-223-3p
Pathways in cancer	4.41E-08	14	2F1,PIK3R2,CHUK,IGF1R,TPM3,IKBKB,CCNE2,MMP1,E2F3,MYC,CDKN1A,IL6,STAT1,VEGF	4	miR-126-3p,miR-145-5p,miR-199a-5p,miR-223-3p
Bladder cancer	7.22E-08	6	E2F1,MMP1,E2F3,MYC,CDKN1A,VEGFA	3	miR-126-3p,miR-145-5p,miR-223-3p
Prostate cancer	1.81E-07	8	E2F1,PIK3R2,CHUK,IGF1R,IKBKB,CCNE2,E2F3,CDKN1A	4	miR-126-3p,miR-145-5p,miR-199a-5p,miR-223-3p
Pancreatic cancer	5.07E-07	7	E2F1,PIK3R2,CHUK,IKBKB,E2F3,STAT1,VEGFA	4	miR-126-3p,miR-145-5p,miR-199a-5p,miR-223-3p
Chronic myeloid leukemia	1.24E-06	7	E2F1,PIK3R2,CHUK,IKBKB,E2F3,MYC,CDKN1A	4	miR-126-3p,miR-145-5p,miR-199a-5p,miR-223-3p
Small cell lung cancer	2.40E-06	7	E2F1,PIK3R2,CHUK,IKBKB,CCNE2,E2F3,MYC	4	miR-126-3p,miR-145-5p,miR-199a-5p,miR-223-3p
HTLV-I infection	0.00015	11	E2F1,PIK3R2,ETS2,CHUK,VCAM1,IKBKB,PPP3CA,E2F3,MYC,CDKN1A,IL6	4	miR-126-3p,miR-145-5p,miR-199a-5p,miR-223-3p
mTOR signaling pathway	0.00022	5	PIK3R2,STK11,IKBKB,IRS1,VEGFA	3	miR-126-3p,miR-145-5p,miR-199a-5p
Glioma	0.00022	5	E2F1,PIK3R2,IGF1R,E2F3,CDKN1A	3	miR-126-3p,miR-145-5p,miR-223-3p
Transcriptional misregulation in cancer	0.00023	8	LMO2,HOXA9,SLC45A3,IGF1R,MYC,CDKN1A,IL6,MEF2C	3	miR-126-3p,miR-145-5p,miR-223-3p
PI3K-Akt signaling pathway	0.00056	12	PIK3R2,IFNB1,STK11,CHUK,IGF1R,IKBKB,CCNE2,MYC,IRS1,CDKN1A,IL6,VEGFA	4	miR-126-3p,miR-145-5p,miR-199a-5p,miR-223-3p
Melanoma	0.00062	5	E2F1,PIK3R2,IGF1R,E2F3,CDKN1A	3	miR-126-3p,miR-145-5p,miR-223-3p
Cytosolic DNA-sensing pathway	0.0007	4	IFNB1,CHUK,IKBKB,IL6	3	miR-145-5p,miR-199a-5p,miR-223-3p
Hepatitis C	0.00123	6	PIK3R2,IFNB1,CHUK,IKBKB,CDKN1A,STAT1	4	miR-126-3p,miR-145-5p,miR-199a-5p,miR-223-3p
Jak-STAT signaling pathway	0.0013	7	PIK3R2,IFNB1,SPRED1,LIF,MYC,IL6,STAT1	4	miR-126-3p,miR-145-5p,miR-199a-5p,miR-223-3p
HIF-1 signaling pathway	0.00137	6	PIK3R2,IGF1R,CDKN1A,IL6,EDN1,VEGFA	4	miR-126-3p,miR-145-5p,miR-199a-5p,miR-223-3p
Measles	0.00162	6	PIK3R2,IFNB1,CHUK,CCNE2,IL6,STAT1	3	miR-126-3p,miR-145-5p,miR-223-3p
Acute myeloid leukemia	0.00266	4	PIK3R2,CHUK,IKBKB,MYC	4	miR-126-3p,miR-145-5p,miR-199a-5p,miR-223-3p
Influenza A	0.00362	6	PIK3R2,IFNB1,MAP2K6,IKBKB,IL6,STAT1	4	miR-126-3p,miR-145-5p,miR-199a-5p,miR-223-3p
Type II diabetes mellitus	0.0043	3	PIK3R2,IKBKB,IRS1	3	miR-126-3p,miR-145-5p,miR-199a-5p
Apoptosis	0.00653	5	PIK3R2,CHUK,DFFA,IKBKB,PPP3CA	4	miR-126-3p,miR-145-5p,miR-199a-5p,miR-223-3p
Adipocytokine signaling pathway	0.00781	4	STK11,CHUK,IKBKB,IRS1	4	miR-126-3p,miR-145-5p,miR-199a-5p,miR-223-3p
Chagas disease (American trypanosomiasis)	0.00902	5	PIK3R2,IFNB1,CHUK,IKBKB,IL6	4	miR-126-3p,miR-145-5p,miR-199a-5p,miR-223-3p
B cell receptor signaling pathway	0.00928	4	PIK3R2,CHUK,IKBKB,PPP3CA	4	miR-126-3p,miR-145-5p,miR-199a-5p,miR-223-3p
Epstein-Barr virus infection	0.01247	6	PIK3R2,CHUK,MAP2K6,IKBKB,MYC,CDKN1A	4	miR-126-3p,miR-145-5p,miR-199a-5p,miR-223-3p
Rheumatoid arthritis	0.0208	3	MMP1,IL6,VEGFA	3	miR-126-3p,miR-145-5p,miR-223-3p
Toxoplasmosis	0.02349	5	PIK3R2,CHUK,MAP2K6,IKBKB,STAT1	4	miR-126-3p,miR-145-5p,miR-199a-5p,miR-223-3p
VEGF signaling pathway	0.04946	3	PIK3R2,PPP3CA,VEGFA	2	miR-126-3p,miR-145-5p
NOD-like receptor signaling pathway	0.04946	3	CHUK,IKBKB,IL6	2	miR-199a-5p,miR-223-3p

Table S5. Functional assessment of miRNAs downregulated in T cells of AA patients

T cell subsets	No stimulation	Control	Anti-miR-126-3p	Anti-miR-145-5p	Anti-miR-126-3p and miR-145-5p
$CD4^+$ Naïve (%)	58.2 ± 4.1	49.4 ± 1.8	47.0 ± 1.8	44.6 ± 1.4	43.4 ± 1.0*
$CD4^+$ TCM (%)	34.8 ± 3.2	40.7 ± 1.3	43.4 ± 1.0	42.4 ± 1.1	43.4 ± 0.7
$CD4^+$ TEM (%)	3.5 ± 0.1	5.7 ± 0.3	5.6 ± 0.4	6.6 ± 0.3	6.8 ± 0.2*
$CD8^+$ Naïve (%)	44.3 ± 0.7	45.1 ± 0.5	45.1 ± 0.4	44.1 ± 0.6	43.1 ± 0.5*
$CD8^+$ TCM (%)	34.8 ± 1.0	36.4 ± 0.3	37.3 ± 0.2	36.0 ± 0.5	36.3 ± 0.3
$CD8^+$ TEM (%)	8.2 ± 0.4	8.1 ± 0.2	8.1 ± 0.3	8.9 ± 0.4	9.2 ± 0.4*

Percentages of Naïve, central memory T cells (TCM), and effector memory T cells (TEM) were examined in $CD4^+$ or $CD8^+$ T cells transfected with anti-miR-126-3p and/or anti-miR-145-5p 48 hours later.
Data are from three independent experiments (means ± SEM). *P < .05 in comparison to control.

Table S6. Functional assessment of miRNAs downregulated in T cells of AA patients

$CD4^+$ T cells	No stimulation	Control	Anti-miR-126-3p	Anti-miR-145-5p	Anti-miR-126-3p and miR-145-5p
GZMB (%)	0.2 ± 0.09	10.5 ± 0.7	16.4 ± 1.4	13.8 ± 2.1	21.6 ± 0.8*
IL-2 (%)	0.1 ± 0.03	30.0 ± 4.8	32.5 ± 6.1	33.2 ± 3.0	45.2 ± 1.4*
IFN- γ (%)	0.1 ± 0.04	11.6 ± 1.5	14.9 ± 3.4	13.1 ± 2.3	23.3 ± 5.0*
$CD8^+$ T cells	**No stimulation**	**Control**	**Anti-miR-126-3p**	**Anti-miR-145-5p**	**Anti-miR-126-3p and miR-145-5p**
GZMB (%)	11.9 ± 1.4	21.0 ± 0.8	24.7 ± 1.7	22.3 ± 0.9	31.0 ± 1.6*
IL-2 (%)	0.3 ± 0.1	10.1 ± 1.3	11.0 ± 1.7	11.7 ± 1.0	14.6 ± 2.7
IFN- γ (%)	0.1 ± 0.02	8.7 ± 3.5	15.1 ± 3.0	13.6 ± 1.0	23.2 ± 0.1*

Percentages of T cells producing GZMB, IFN-γ, and IL-2 were examined in $CD4^+$ or $CD8^+$ T cells transfected with anti-miR-126-3p and/or anti-miR-145-5p 48 hours later.

Data are from three independent experiments (means ± SEM). *P < .05 in comparison to control.

Table S7. Quantitative PCR primer list

Name	Catalog number
hsa-miR-126-3p	MS00003430
hsa-miR-145-5p	MS00003528
hsa-miR-199a-5p	MS00006741
hsa-miR-223-3p	MS00003871
RNU-2	MS00033740
MYC	PPH00100B-200
PIK3R2	PPH00709A-200
ETS1	PPH01781C-200
FOXO1	PPH01964F-200
HIF1A	PPH01361B-200
PARP1	PPH00686B-200
PAK4	PPH08265A-200
PLK2	PPH19054G-200
b-actin	PPH00073G-200

A **Gating strategy for sorting of human lymphocyte subsets**

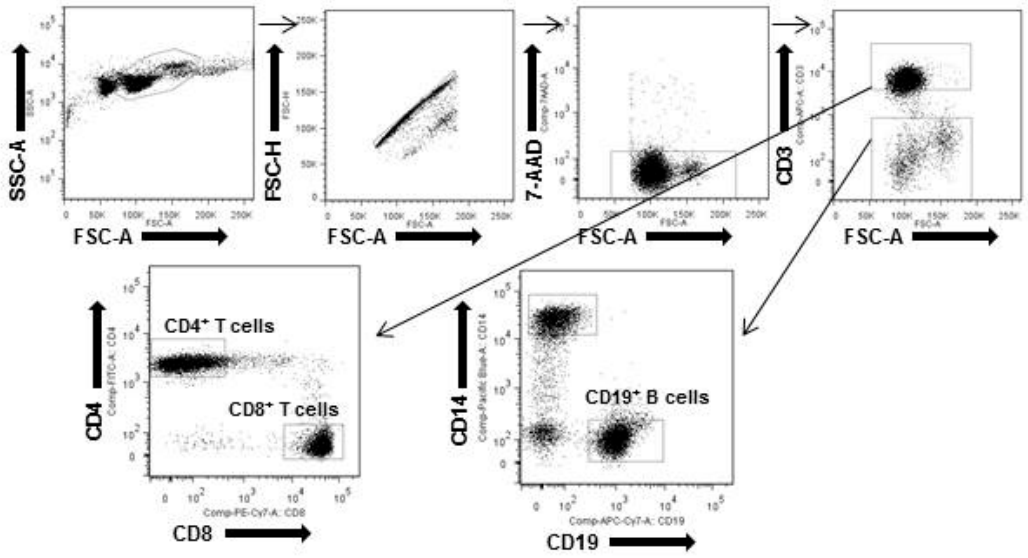

B **Gating strategy for sorting of human T cell subsets**

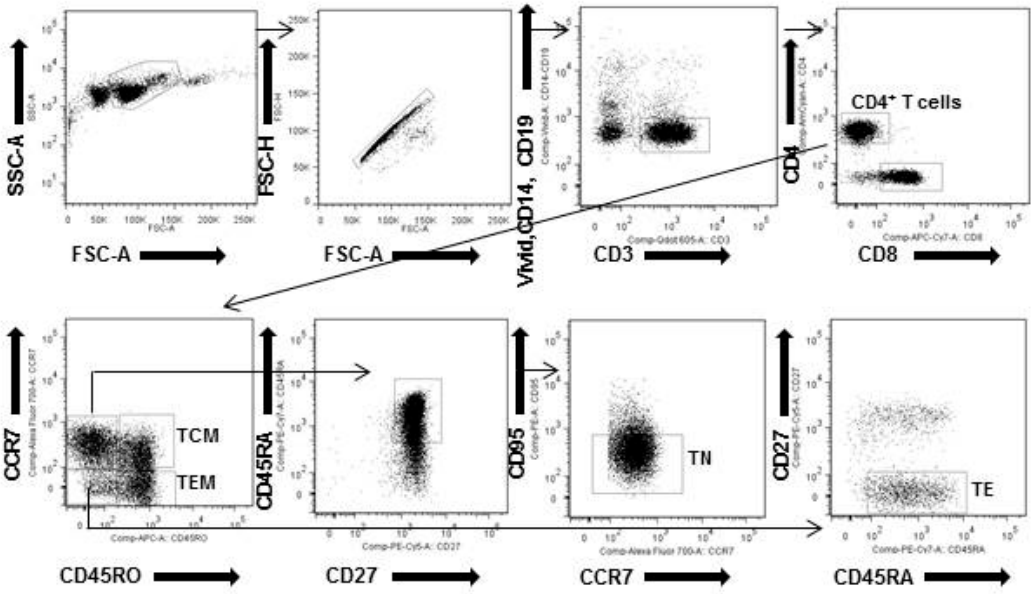

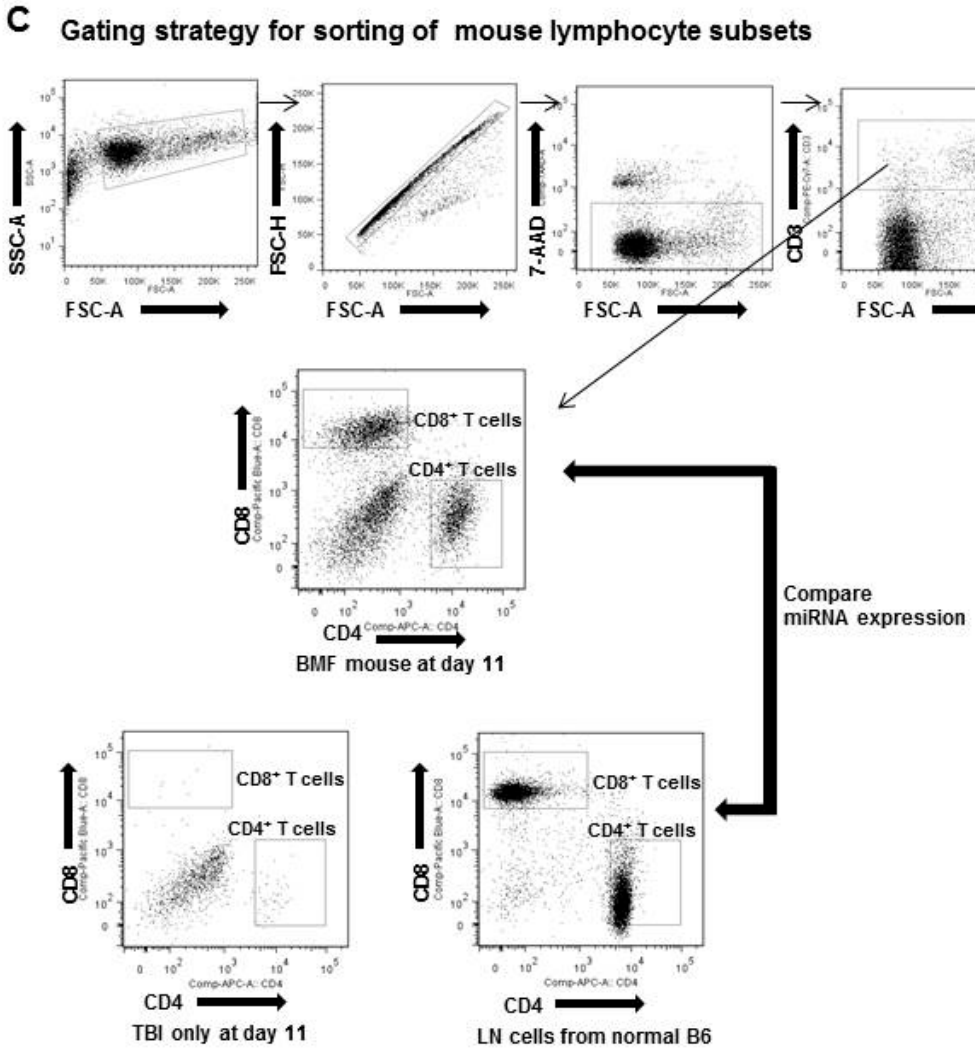

Figure S1. Gating strategy for sorting human and mouse lymphocyte subsets and human T cell subsets. (A) Human PBMCs were stained with anti-CD4-FITC, anti-CD3-APC, anti-CD8-PE-Cy7, anti-CD19-APC-Cy7, anti-CD14-Pacific Blue, and anti-CD28-PE. $CD4^+$ T cells, $CD8^+$ T cells, $CD19^+$ B cells, and $CD14^+$ monocytes were identified as shown in Figure 1A. Mononuclear cells were first gated based on forward- and side-scatter characteristics; single cells were gated based on forward scatter height vs. forward scatter area; and live T cells were gated based on expression of CD3 without staining for the dead cell dye 7-AAD. $CD4^+$ and $CD8^+$ T cells were then gated from $CD3^+$ cells.

$CD19^+$ B cells and $CD14^+$ monocytes were gated from $CD3^-$ cells. (B) Human PBMCs were stained with ViViD, anti-CD14-Pacific Blue, anti-CD19-Pacific Blue, anti-CD3-BV605, anti-CD4-V500, anti-CD8-APC-H7, anti-CD45RA-PE-Cy7, anti-CD45RO-APC, anti-CCR7-AF700, anti-CD27-PC5, and anti-CD95-PE. $ViViD^-CD3^+$ CD4 $(CD8)^+$ $CD45RO^-$ $CD45RA^+$ $CCR7^+$ $CD27^+$ $CD95^-$ TN, $ViViD^-CD3^+$ CD4 $(CD8)^+$ $CD45RO^+$ $CCR7^+$ TCM, $ViViD^-$ $CD3^+$ CD4 $(CD8)^+$ $CD45RO^+$ $CCR7^-$ TEM, and $ViViD^-CD3^+$ CD4 $(CD8)^+$ $CD45RO^-$ $CD45RA^+$ $CCR7^-$ $CD27^-$ TE were identified as shown in figure 1B. Lymphocytes were gated based on their scatter characteristics, and single lymphocytes were gated based on forward scatter height vs. forward scatter area. Live T cells were gated based on positive for CD3 and negative for ViViD, CD14, and CD19 to remove dead cells, monocytes, and B cells. $CD4^+$ and $CD8^+$ T cells are then gated based on the characteristic expression patterns of CCR7 and CD45RO.

(C) Mouse BM cells were stained with anti-CD4-APC, anti-CD3-PE-Cy7, anti-CD8-Pacific Blue, anti-CD45R-APC-Cy7, anti-CD11b-FITC, and anti-Gr1-PE. $CD4^+$ and $CD8^+$ T cells were identified as shown in figure 1C. Normal B6 LNs were sorted to compare miRNA expression profiles, due to low cell numbers of $CD4^+$ and $CD8^+$ T cells from mice which were received 5 Gy TBI-only without LN cell infusion.

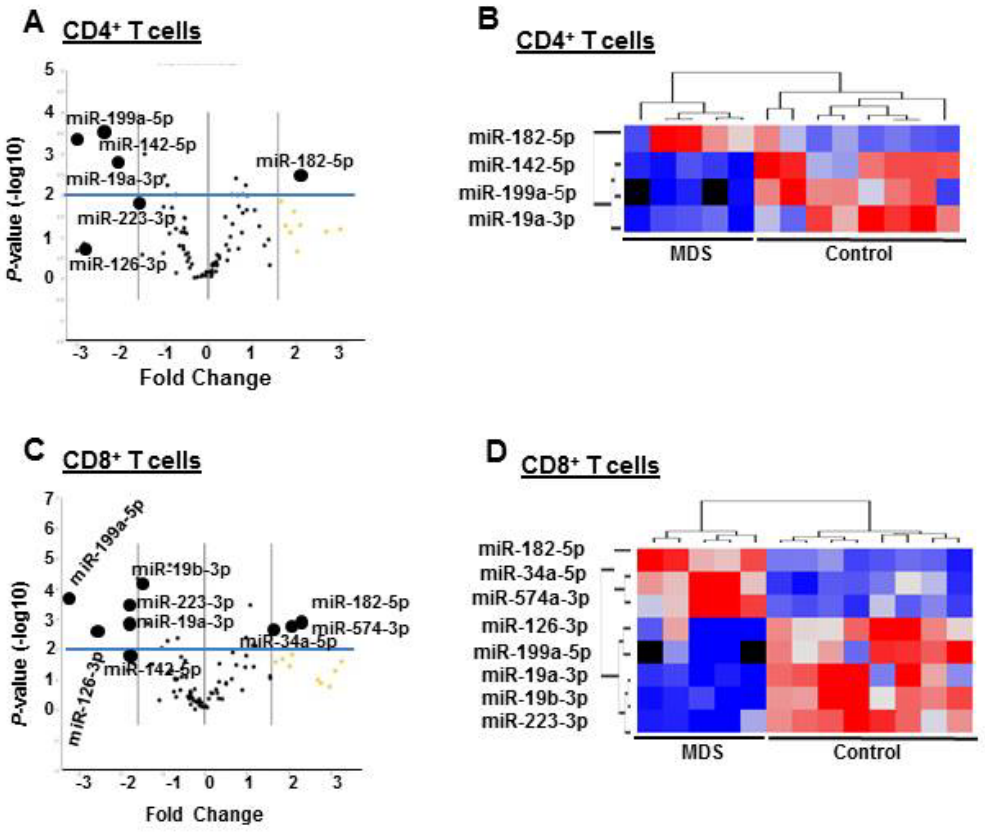

Figure S2. Distinct patterns of miRNA expression in CD4$^+$ and CD8$^+$ T cells of low-risk MDS patients. Volcano plots of 84 miRNA relative expression levels known to be involved in lymphocyte activation in CD4$^+$ (A) and CD8$^+$ (C) T cells from patients with low-risk MDS (n = 5) and healthy donors (n = 8) using miRNA PCR-array. The x-axis is an estimated difference in expression measured in log2, and vertical lines indicate a 3-fold expression difference between the two groups. MiRNAs highly expressed in MDS or healthy donors are on the right or the left, respectively. The y-axis is the significance of the difference measured in −log10 of the *P*-value and the horizontal line represents our cutoff for significance at $P < .01$. Hierarchical clustering of CD4$^+$ (B) or CD8$^+$ (D) T cells was performed by analyzing differentially expressed miRNA between the two groups. A red-blue color scale depicts normalized miRNA expression levels in Ct values (red: high, blue: low).

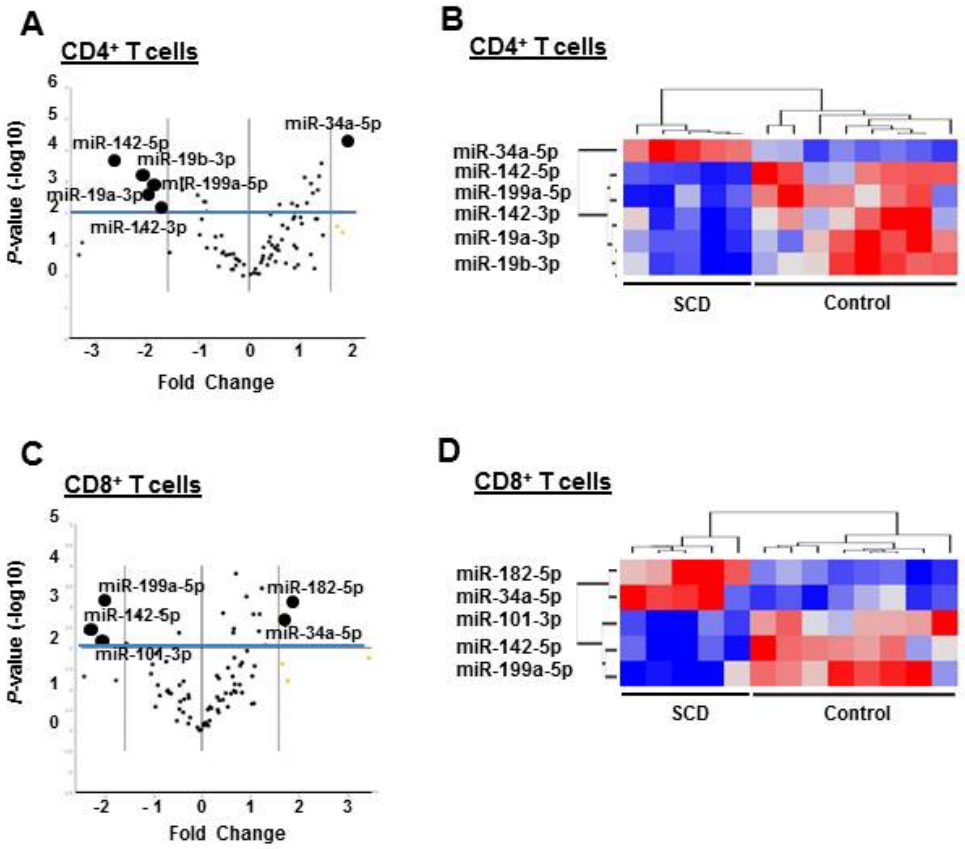

Figure S3. Distinct pattern of miRNA expression in CD4$^+$ and CD8$^+$ T cells of SCD patients. Volcano plots of 84 miRNA relative expression levels in CD4$^+$ (A) and CD8$^+$ (C) T cells from SCD patients (n = 5) and healthy donors (n = 8) using miRNA PCR-array. The x-axis is an estimated difference in expression measured in log2 and vertical dotted lines refer to a 3-fold difference in expression between the two groups. MiRNAs highly expressed in SCD or healthy donors are on the right or the left, respectively. The y-axis is the significance of the difference measured in −log10 of the *P*-value and the horizontal line represents our cutoff for significance at $P < .01$. Hierarchical clustering of CD4$^+$ (B) or CD8$^+$ (D) T cells was performed by analyzing differentially expressed miRNAs between the two groups. A red-blue color scale depicts normalized miRNA expression levels in Ct values (red: high, blue: low).

Supplemental Figure 4, Hosokawa et al.

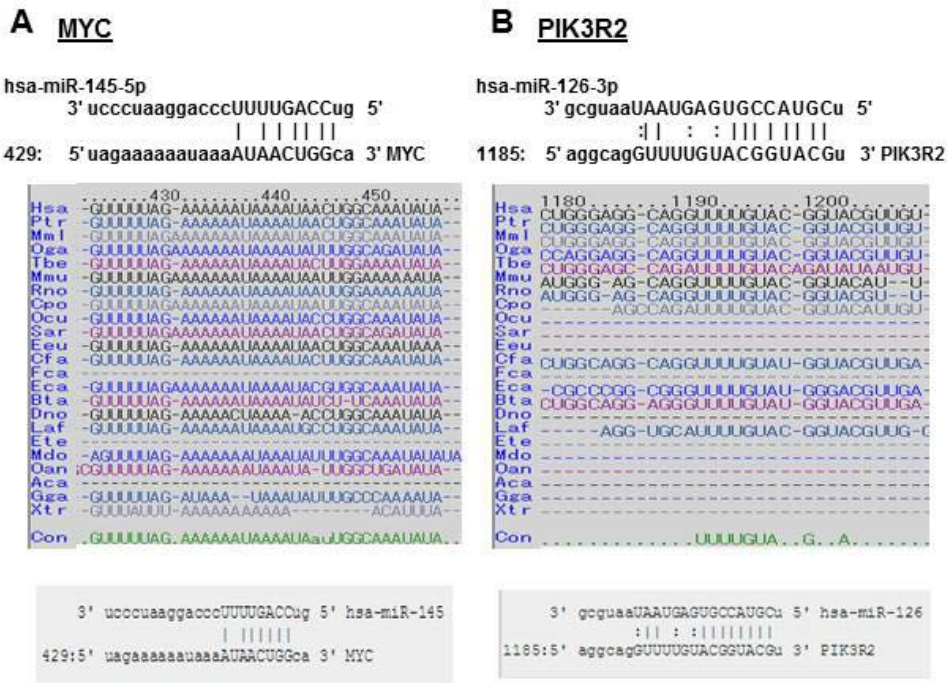

Figure S4. Target sequences of miR-145-5p in MYC 3′ UTRs or miR-126-3p in PIK3R2 3′ UTRs in various species. MiR-145-5p target sequences in MYC 3′ UTRs (A) and miR-126-3p target sequences in PIK3R2 3′ UTRs (B) in various species were identified by TargetScan prediction. Genetic conservation in miR-145-5p and miR-126-3p targeting regions were observed beyond species.

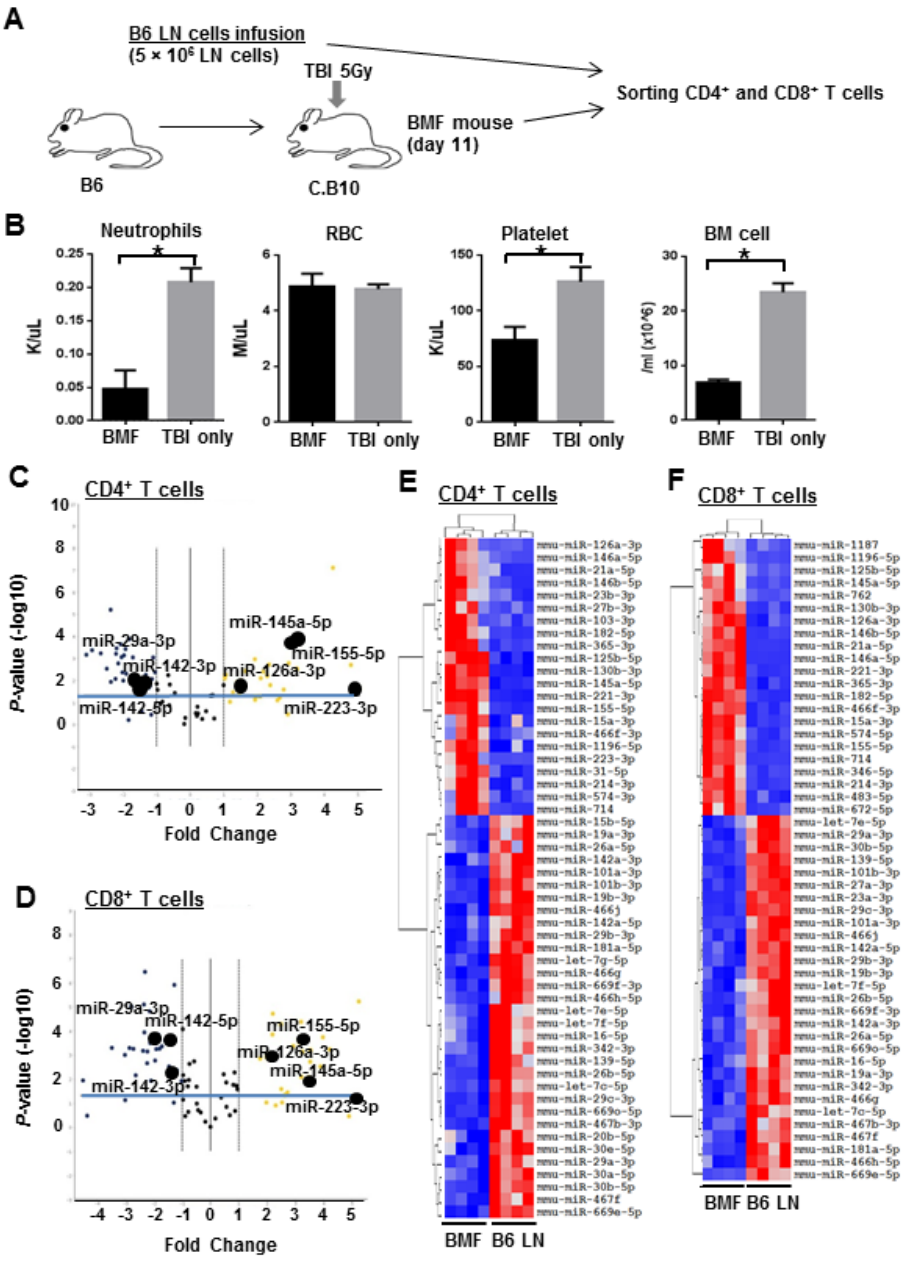

Figure S5. T cells from LN cell infusion-induced BMF mice show distinct miRNA profiles.

(A) Experimental design was summarized. (B) Four recipient mice received B6 LN cells had severe neutropenia, thrombocytopenia, and reductions in total BM cells. Volcano plots were illustrated 84 miRNA relative expression levels in $CD4^+$ (C) and $CD8^+$ (E) T cells sorted from BM of BMF mice (n = 4) by comparison with normal B6 LN cells (n = 4). The x-axis

represents an estimated expression difference measured in log2; vertical lines show a 2-fold expression difference between the two groups. MiRNAs highly expressed in BM T cells of BMF mice or in T cells of B6 LN cells are on the right or the left, respectively. The y-axis is significant difference measured in −log10 of the *P*-value; the horizontal line represents our cutoff for significance at $P < .05$. Hierarchical clustering of $CD4^+$ (D) or $CD8^+$ (F) T cells was performed analyzing miRNAs which were found differentially expressed between the two groups. A red-blue color scale depicts normalized miRNA expression levels in Ct values (Red: high, Blue: low). $*P < .05$ (Student's t-test).

Supplemental Figure 6, Hosokawa et al.

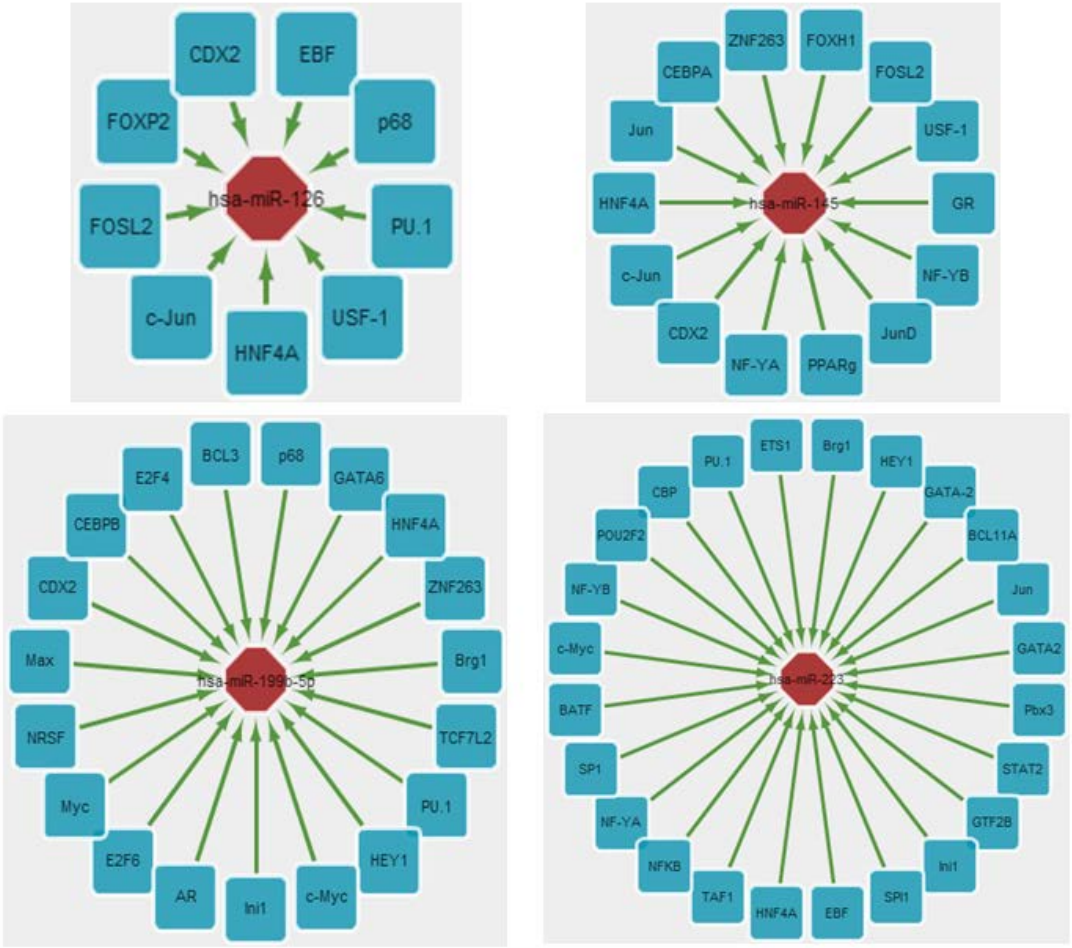

Figure S6. Transcription factor networks.

ChIPBase is an integrated resource and platform for decoding transcription factor (TF) binding maps, expression profiles, and transcriptional regulation of long non-coding RNAs (lncRNAs, lincRNAs), miRNAs, from ChIP-Seq data. Four miRNAs share the commnon transcriptional factors. Brown octagons and green rectangles denote miRNAs and TFs, respectively.

Supplemental Experimental Methods

Mononuclear Cell Separation

Peripheral blood samples were collected after informed consent was obtained in accordance with the Declaration of Helsinki and research protocol approved by the NHLBI Institutional Review Board. Peripheral mononuclear cells (PBMCs) were separated by density gradient centrifugation at 500g for 25 minutes at room temperature using LSM lymphocyte separation medium (MP Biomedicals LLC, Santa Ana, CA) and cryopreserved in RPMI-1640 (Life Technologies, Gaithersburg, MD) supplemented with 20% heat-inactivated fetal bovine serum (Sigma-Aldrich, St Louis, MO) and 10% dimethyl sulfoxide according to standard protocols until use.

Flow Cytometry and Cell Sorting

For RNA extraction, PBMCs from patients with AA, low-risk MDS, SCD, and healthy donors were sorted for $CD4^+$ T cells, $CD8^+$ T cells, $CD3^-$ $CD19^+$ B cells, and $CD3^-$ $CD14^+$ monocytes by fluorescence-activated cell sorter on an Aria II instrument (Becton Dickinson, Franklin Lakes, NJ). For T cell subset analysis, PBMCs were stained with ViViD, CD3-BV605, CD4-V500, CD8-APC-H7, CD45RA-PE-Cy7, CD45RO-APC, CCR7-AF700, CD27-PC5,and CD95-PE to sort ViViD$^-$$CD3^+$ CD4 $(CD8)^+$ $CD45RO^-$ $CD45RA^+$ $CCR7^+$ $CD27^+$ $CD95^-$ naïve T cells (TN), ViViD$^-$ $CD3^+$ CD4 $(CD8)^+$ $CD45RO^+$ $CCR7^+$ central memory T cells (TCM), ViViD$^-$ $CD3^+$ CD4 $(CD8)^+$ $CD45RO^+$ $CCR7^-$ effector memory T cells (TEM), and ViViD$^-$ $CD3^+$ CD4 $(CD8)^+$ $CD45RO^-$ $CD45RA^+$ $CCR7^-$ $CD27^-$ terminally-differentiated effectors T cells (TE).

For mouse study, BM cells from BMF mice and lymph node (LN) cells from normal C57BL/6J (B6) mice were sorted for $CD4^+$ T cells, $CD8^+$ T cells, $CD3^-$ $CD45R^+$ B cells, and $Gr1^+$ monocytes by flow cytometry using an Aria II instrument for RNA extraction. Gating

strategy for sorting lymphocyte subsets in human or mouse samples, and T cell subsets in human samples are summarized in supplemental Figure1. Each cell population was obtained at purity of 99%.

Fluorochrome-conjugated monoclonal antibodies (mAbs) were purchased from commercial vendors: anti-CD4-FITC, anti-CD14-Pacific Blue, and anti-CD28-PE (BD Biosciences, San Diego, CA); and anti-CD3-APC, anti-CD8 PE-Cy7, anti-CD19-APC-Cy7, and anti-CD14-Pacific Blue (Biolegend, San Diego, CA). For T cell subset staining, the following antibodies were used: anti-CD4-V500, anti-CD8-APC-H7, anti-CD45RA-PE-Cy7, anti-CD45RO-APC, anti-CCR7-AF700, and anti-CD95-PE (BD Biosciences); anti-CD3-BV605 (Biolegend); anti-CD14-Pacific Blue and anti-CD19-Pacific Blue (Invitrogen, Carlsbad, CA); and anti-CD27-PC5 (Beckman Coulter, Indianapolis IN). The fixable violet amine reactive dye (ViViD; Invitrogen/Molecular Probes, Eugene, OR) or Via-Probe (7AAD; BD Biosciences) was used to eliminate dead cells from the analysis. For intracellular cytokine staining, following antibodies were used as well as surface staining: anti-granzyme B (GZMB)-FITC, anti-IL-2-FITC and anti- IFN -γ –FITC (BD Biosciences). For mouse sample staining, the following mAbs were obtained from commercial vendors: anti-CD11b-FITC, anti-Gr1-PE, anti-7AAD, anti-CD3-PE-Cy7, anti-CD4-APC, anti-CD45R-APC-Cy7, and anti-CD8-Pacific Blue (all BD Biosciences).

Quantitative real-time RT-PCR (RT-qPCR)

RT-qPCR was performed for validation of miRNA expression. Briefly, reverse transcription was performed on an equal amount of RNA for each sample, using the miScript II RT kit with HiSpec buffer (QIAGEN), followed by RT-qPCR using the miScript SYBR Green PCR kit (200) (QIAGEN) with adequate primers, with analysis by the ABI Prism 7900HT Sequence Detection System (Applied Biosystems, Grand Island, NY). Amplification conditions of

qPCR were an initial hold at 95°C for 15 min followed by 40 cycles of 94°C for 15 sec, 55°C for 30 sec, and 70°C for 30 sec. All PCR reactions were in triplicate, and miRNA expression relative to control RNU-2 was calculated using the 2−ΔΔCt method.

For validation of mRNA expression, reverse transcription of mRNAs was performed on an equal amount of RNA for each sample using the RT² First Strand kit (QIAGEN). SYBR Green incorporation RT-qPCR was performed using RT² SYBR Green ROX qPCR Mastermix (QIAGEN) and analyzed by the ABI Prism 7900HT Sequence Detection System: an initial hold at 95°C for 10 min, followed by 40 cycles of 95°C for 15 sec and 60°C for 60 sec. All PCR reactions were in triplicate, and mRNA expression relative to control β-actin was calculated using the 2−ΔΔCt method. Real-time PCR primers are listed in supplemental Table 7.

Target prediction and pathway analysis

Putative target genes regulated by differentially expressed miRNAs in AA were predicted bioinformatically using the miRBase (http://www.mirbase.org), PicTar (http://pictar.bio.nyu.edu), TargetScan version 6.2 (http://www.targetscan.org/index.html), and miRTarBase (http://mirtarbase.mbc.nctu.edu.tw) search engines and the Ingenuity Knowledge Base (IPAKB). To optimize the accuracy of prediction, a potential gene target should be predicted by a minimum of two out of four programs, and further a targeted sequence should be conserved across species. To identify molecular pathways potentially altered by the expression of multiple miRNAs, we used the DIANA-mirPath web-based computational tool.[1]

Cell purification and functional assays

PBMCs from healthy donors or AA patients were isolated by density-gradient centrifugation, and human $CD4^+$ and $CD8^+$ T cells were purified by positive selection with anti-CD4 and anti-CD8–coated MACS magnetic beads (Miltenyi, San Diego, CA), respectively. Purity of all cell preparations was >90%. Cells were cultured in RPMI 1640 medium (Life Technologies) containing 10% FBS and 1% penicillin/streptomycin. For transfection, $CD4^+$ and $CD8^+$ T cells were seeded in 24-well plates with 1×10^6 cells/well. Using the Human T Cell Nucleofector R kit (Lonza AG, Allendale, NJ), freshly isolated $CD4^+$ and $CD8^+$ T cells were transfected with 100 pmol of miR-126-3p or miR-145-5p mimic or inhibitor/10^6 cells (mirVana miRNA mimic or Inhibitor, assay ID MH12841 and MH11480, Applied Biosystems), and 100 pmol of negative control (mirVana miRNA mimic or inhibitor Negative Control No. 1, Applied Biosystems). These inhibitory antagomirs were tentatively termed anti-miR-126-3p and anti-miR-145-5p, respectively, in this study and their target sequences were as follows:

miR-126-3p: 5'- UCGUACCGUGAGUAAUAAUGCG–3' and

miR-145-5p: 5'- GUCCAGUUUUCCCAGGAAUCCCU–3'.

Transfection efficiency was around 70%, as assessed by flow cytometry, for a cotransfected GFP reporter. The medium was changed 4 hours postelectroporation, and T cells were activated with Dynabeads® Human T-Activator CD3/CD28 for physiological activation of human T cells (Life technologies). To assess the effects of miRNA knockdown on miRNA, mRNA, and protein expression, and cell functions, RT-qPCR, immunoblot, intracellular cytokine staining, and CFSE cell proliferation assay were performed 24, 48, 48, and 96 hours postelectroporation.

CFSE assay

After cell separation, cells were labeled by the CellTrace™ CFSE Cell Proliferation kit (Invitrogen) and subjected to electroporation of miRNA mimic or inhibitors. A total of 2×10^5 CFSE-labelled cells were cultured in 24-well plate with Dynabeads® Human T-Activator CD3/CD28. After 96 hours, acquisition was conducted on LSR II (BD Biosciences) and data were analyzed using FlowJo software (FlowJo, Ashland, OR).

Immunoblot

Expression levels of *MYC* and *PIK3R2* were analyzed by immunoblot 48 hours postelectroporation. Briefly, cells were lysed with M-PER Mammalian Protein Extraction Reagent (Thermo Scientific, West Palm Beach, FL) with a proteinase inhibitor mixture (Roche, Nutley, NJ). Cell lysate (10 μg of protein) was separated by 10% sodium dodecyl sulphate polyacrylamide gel electrophoresis and transferred onto a PVDF membrane (Invitrogen). For immunoblotting, anti-MYC rabbit mAb (1:1000; D84C12, Cell Signaling, Danvers, MA), anti-PI3 Kinase p85 (PIK3R2) rabbit mAb (1:1000; Cell Signaling), or anti-β-actin goat polyclonal antibody (1:100; I-19; Santa Cruz Biotechnology, Santa Cruz, CA) was used as primary antibody, and anti-mouse IgG conjugated with a horseradish peroxidase (HRP), anti-rabbit IgG-HRP, or anti-goat IgG-HRP was used as secondary antibody (Santa Cruz). The signals were visualized by enhanced chemiluminescence (Thermo Scientific).

Dual luciferase assay

Transient transfections of $CD4^+$ and $CD8^+$ T cells were performed by using the Human T Cell Nucleofector R kit (Lonza AG, Allendale, NJ) according to the manufacturer's instructions. For the luciferase assay, cells were seeded in 24-well plates with 1×10^6 cells/well and co-transfected with either 3 μg of MiTarget MicroRNA 3' UTR Target Clone

HmiT067350-MT06 (GeneCopoeia, *MYC* 3’ UTR) or HmiT013158-MT06 (GeneCopoeia, *PIK3R2* 3’ UTR), as well as 100 pM miRNA mimics (miR-145-5p for *MYC* 3’ UTR, and miR-126-3p for *PIK3R2* 3’ UTR, respectively) per well. Control wells were transfected with either HmiT067350-MT06 or HmiT013158-MT06 plasmid, and negative control (mirVana miRNA mimic Negative Control No. 1, Applied Biosystems). HmiT067350-MT6 and HmiT013158-MT06 plasmids express both firefly and renilla luciferase. Firefly and renilla luciferase activities were measured 24 hours after transfection by using the Luc-Pair™ luciferase assay kit (GeneCopoeia) and a victor3 1420 multilabel counter (PerkinElmer). Firefly luciferase activity was normalized to renilla luciferase activity for each transfected well. In all the experiments, transfection and luciferase assays were performed in triplicate.

Intracellular cytokine staining

Expression levels of GZMB, IL-2 and IFN- γ were analyzed by intracellular cytokine staining 48 hours postelectroporation. Briefly, cells were stimulated with Dynabeads® Human T-Activator CD3/CD28 with Golgi transport inhibitor, which was present for the final 4 h of culture. Cells were fixed, permeabilized, and stained using Cytofix/Cytoperm Fixation/Permeabilization solution kit with GolgiPlug (BD Biosciences) according to the manufacturer's protocol.

Mouse study

Inbred B6 and congenic C.B10-H2(b)/LilMcd (C.B10) mice, obtained from the Jackson Laboratory, were bred and maintained in the National Institutes of Health animal facility under standard care and nutrition. All animal studies were approved by the National Heart, Lung, and Blood Institute's Animal Care and Use Committee. Mice were 2 to 6 months of age and sex-matched between donors and recipients in each experiment. Cells from inguinal,

brachial, and axillary LNs of B6 donors were homogenized with tissue grinder, and were filtrated through 90 μM nylon mesh to produce single-cell suspensions. For the induction of BMF, B6 LN cells were infused into C.B10 mice at 5×10^6 cells/ recipient, as previously described.[2] All recipient mice received a sublethal dose of 5 Gy total body irradiation (TBI) from a Shepherd Mark 1 137 cesium γ irradiator (J. L. Shepherd) 4-6 hours before cell infusion. In each experiment, mice received 5 Gy TBI-only without LN cell infusion were used as experiment controls. Animals were bled at 11 days after LN cell infusion, by retro-orbital sinus bleeding, for complete blood counts (CBCs) using a Hemavet 950 analyzer (Drew Scientific). Animal were then euthanized to extract BM cells from bilateral femurs and tibiae followed by cell sorting for RNA extraction. For comparison of miRNA expression levels, LN cells from age and sex-matched B6 donors were used as controls.

In silico analysis of transcription factor miRNA interaction

The transcription factor and miRNA relationship data were extracted from the ChIPBase.[3] ChIPBase aims to provide high confident information on the transcriptional regulation of long non-coding RNA and miRNA genes from ChIP-Seq data.

Statistics

All statistical analyses were done using GraphPad PRISM version 6.0 (GraphPad Software, Inc., La Jolla, CA, USA). All experiments were performed in triplicates. Data was represented as means ± SEM (Standard Error of Means). Student's t test was used to calculate statistical significance between two groups. ANOVA was used for statistical analysis of the multiple groups. A two-tailed P value < 0.05 was considered statistically significant.

Supplemental References

1. Vlachos IS, Kostoulas N, Vergoulis T, et al. DIANA miRPath v.2.0: investigating the combinatorial effect of microRNAs in pathways. Nucleic Acids Res. 2012;40(Web Server issue):W498-504.

2. Chen J, Ellison FM, Eckhaus MA, et al. Minor antigen h60-mediated aplastic anemia is ameliorated by immunosuppression and the infusion of regulatory T cells. J Immunol. 2007;178(7):4159-4168.

3. Yang JH, Li JH, Jiang S, Zhou H, Qu LH. ChIPBase: a database for decoding the transcriptional regulation of long non-coding RNA and microRNA genes from ChIP-Seq data. Nucleic Acids Res. 2013;41(Database issue):D177-187.